Thin Solid Films 520 (2012) 6057–6063

Contents lists available at SciVerse ScienceDirect

Thin Solid Films

journal homepage: www.elsevier.com/locate/tsf

Investigation of the microstructure, mechanical properties and tribological behaviors of Ti-containing diamond-like carbon films fabricated by a hybrid ion beam method

Wei Dai [a,b], Peiling Ke [a], Myoung-Woon Moon [b], Kwang-Ryeol Lee [b], Aiying Wang [a,*]

[a] Ningbo Key Laboratory of Marine Protection Materials, Division of Surface Engineering, Ningbo Institute of Materials Technology and Engineering, Chinese Academy of Sciences, Ningbo 315201, PR China
[b] Future Convergence Technology Division, Korea Institute of Science and Technology, Seoul, 130-650, Republic of Korea

ARTICLE INFO

Article history:
Received 21 October 2011
Received in revised form 31 March 2012
Accepted 5 April 2012
Available online 16 April 2012

Keywords:
Diamond-like carbon
Titanium doping
Mechanical property
Tribology
Hybrid ion beam deposition
Transmission electron microscopy

ABSTRACT

Diamond-like carbon (DLC) films with various titanium contents were investigated using a hybrid ion beam system comprising an anode-layer linear ion beam source and a DC magnetron sputtering unit. The film composition and microstructure were characterized carefully by X-ray photoelectron spectroscopy, transmission electron microscopy and Raman spectroscopy, revealing that the doped Ti atoms had high solubility in the DLC films. The maximum solubility was found to lie between about 7 and 13 at.%. When the Ti content was lower than this solubility, the doped Ti atoms dissolved in the DLC matrix and the films exhibited the typical features of the amorphous DLC structure and displayed low compressive stresses, friction coefficients and wear rates. However, as the doped content exceeded the solubility, Ti atoms bonded with C atoms, resulting in the formation of carbide nano-particles embedded in the DLC matrix. Although the emergence of the carbide nano-particles promoted graphitizing due to a catalysis effect, the film hardness was enhanced to a great extent. On the other hand, the hard carbides particles caused abrasive wear behavior, inducing a high friction coefficient and wear rate.

1. Introduction

Diamond-like carbon (DLC) films have potential widespread applications in many industrial fields, such as applications in cutting tools and dies, magnetic data storage, micro-electromechanical devices, biological implants, and solar cells, due to their outstanding properties which include high hardness, low friction coefficient, good anti-corrosion properties and bio-compatibility with the human body, smooth surfaces, and optical transparency [1–3]. However, the existence of high compressive stress in DLC films, which arises from the deposition mechanism known as sub-plantation, leads to poor adhesion of the films to the substrates and limits the extended utilization of DLC films [4–6]. Metal element doping has been considered as one of the most effective methods for reducing compressive stress and strengthening film adhesion to the substrate [7,8]. In addition, the doping metal atoms could create a two-dimensional array of nano-clusters within the DLC matrix or an atomic-scale composite dissolved in the DLC matrix, which would significantly influence the mechanical and tribological properties [9,10]. Singh et al. [9] reported on Cr incorporated into DLC films by a hybrid physical vapor deposition and plasma-enhanced chemical vapor deposition (PECVD) and found that films with low Cr content showed similar mechanical and tribological characteristics to those of pure DLC films, while films with high Cr content exhibited high hardness and abrasive wear behavior due to the hard carbide phases embedded in the DLC matrix. Furthermore, the formation of composite structures was supposed to strongly depend on the doped metal solubility in the DLC matrix, which was significantly correlated with the nature and content of the doping metal as well as the deposition technique and the process parameters. This indicates that the microstructure and properties of DLC films can be thus tailored for multifunctional applications by varying the nature and level of the doping metal.

Titanium is considered to be a strong candidate element for reducing DLC compressive stress, which can modify the mechanical, tribological and biological properties of the DLC films [11–13]. Several methods have been used to deposit Ti-containing DLC (Ti-DLC) film, such as reactive magnetron sputtering [14], co-sputtering of graphite and titanium targets [15] and the PECVD technique [16]. In the present paper, we obtained the Ti-DLC films using a hybrid ion beam system comprising an anode-layer linear ion beam source for carbon and DC magnetron sputtering for Ti, which can easily vary the Ti doping content in a wide range from <4 up to 24 at.%. The composition and microstructure of the Ti-containing DLC films were carefully studied by X-ray photoelectron spectroscopy (XPS), transmission electron microscopy (TEM) and Raman spectroscopy. The compressive stress and mechanical properties, including the elastic modulus and hardness of the Ti-DLC films, were measured by using a stress-tester and by nanoindentation, respectively. A ball-on-disc tribo-tester was used for the characterization of

* Corresponding author.
E-mail address: aywang@nimte.ac.cn (A. Wang).

0040-6090/$ – see front matter © 2012 Elsevier B.V. All rights reserved.
doi:10.1016/j.tsf.2012.04.016

the tribological behavior of the films as a function of doped Ti content, and the related mechanisms were discussed in terms of the film microstructure.

2. Experimental details

Silicon (100) wafers with a thickness of 525 ± 15 μm were used as the substrates, which were cleaned ultrasonically in acetone and ethanol and dried in air before being put into the vacuum chamber. In addition, 285 ± 5 μm thick silicon wafer strips of size 3 mm × 35 mm were used as the substrates to accurately estimate the in-plane compressive stress. Ti-DLC films were deposited by a linear anode-layer ion source (LIS) [17] combined with a DC magnetron sputtering unit. The LIS with a cross-sectional area of about 100 mm (width) × 380 mm (length) faces to the substrate at an angle of 20°. And the magnetron sputtering unit equipped with a 100 mm (width) × 380 mm (length) rectangular titanium target (99.99%), also is put to the substrate at an angle of 20°. The distance between the substrate and the LIS as well as the magnetron sputtering unit is about 200 mm. A schematic of the preparation process may be referred to in the previous works [18,19]. Acetylene gas of 10 sccm was introduced into the LIS to obtain the hydrocarbon ions. Typical values of the discharge voltage and current of the linear ion source were 1650 V and 0.2 A, respectively. Argon gas of 70 sccm was supplied to the magnetron sputtering unit. DC power (under current control mode) with various currents in the range of 2–3 A was supplied to the magnetron sputtering unit to control the doped Ti content in the films. During the film deposition, the working pressure was kept around 0.5 Pa, and a pulse negative bias voltage of −50 V (350 kHz, 1.1 μs) was supplied to the substrates. The deposition time was maintained at 1 h.

The thicknesses of the deposited films were measured using a surface profilometer (Alpha-step IQ, US) on a step between the films and Si wafer covered with a shadow mask. The film thicknesses were estimated to range from 800 to 1200 nm in the present experiment. The composition and chemical bonds of the Ti-DLC films were analyzed by XPS (Axis ultraDLD) with Al (mono) Kα irradiation at a pass energy of 160 eV. Before commencing the measurement, an Ar^+ ion beam with an energy of 2 keV was used to etch the sample surface for 5 min to remove any contaminants. The relative Ti/C atomic ratio of the films was determined based on the atomic sensitivity factors and area ratio of the C 1s to Ti 2p peaks in XPS spectra of the films. For simplicity, the hydrogen content in the films was neglected due to the lack of signal intensity in the current XPS detection measurement. High-resolution TEM of the DLC films was performed using a Tecnai F20 electron microscope (FEI company, Netherlands), which was operated at 200 keV with a point-to-point resolution of 0.24 nm. The specimens for TEM analysis were directly deposited on freshly cleaved single-crystal NaCl wafers with thicknesses of about 80 nm, and afterwards were peeled off by dissolving the NaCl wafers in deionized water. Raman spectroscopy with an incident Ar^+ beam at a wavelength of 514.5 nm was used to assess the carbon atomic bond structure in the films.

The in-plane compressive stress of the films was calculated from the curvature of the film/substrate composite using the Stoney equation, where the curvature of the film/substrate composite was determined by a laser tester. The hardness and elastic modulus were measured by the nano-indentation technique in a continuous stiffness measurement mode with a maximum indentation depth of 500 nm. The characteristic hardness of the films was chosen to be that which was measured at a depth of around 1/10 of the film thickness in order to minimize the substrate contribution. Six replicate indentations were operated for each sample. The tribological behaviors of the films were investigated using a rotary ball-on-disk tribometer at room temperature with a relative humidity of about 50% under dry sliding conditions. A steel ball (SUJ-2, HRC60) with a diameter of 7 mm was used as the counter body. All the tests were performed at 0.1 ms^{-1} sliding velocity over a distance of 300 m with an applied load of 3 N. After the friction test, the morphologies of the wear tracks were analyzed by a 3D scanning surface profiler (AEP, US) and the wear scars of the counter balls were studied by using an optical microscope (Leica DM2500 M, German). Detailed images of the wear track were taken using a scanning electronic microscope (SEM) (S4800, Hitachi, Japan) at 15 keV operating voltage. An energy dispersive spectrometer (EDS) with an accelerating voltage of 20 keV was also used for compositional analysis.

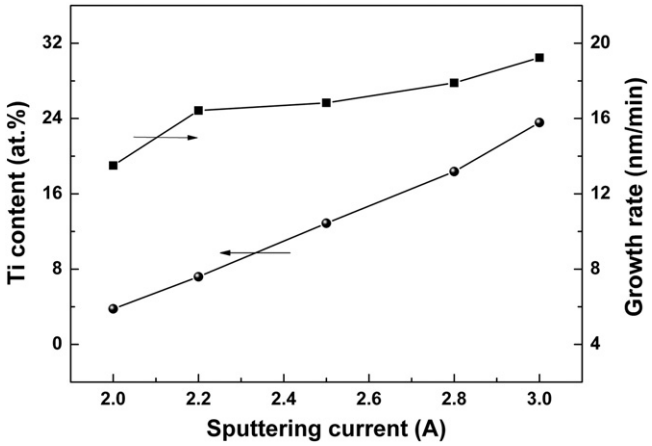

Fig. 1. Ti content and growth rate of the Ti-DLC films as a function of the sputtering current.

3. Results and discussion

The Ti contents and growth rates of the as-deposited films are shown in Fig. 1 as a function of the magnetron sputtering current. It can be seen that the Ti content in the films increased linearly with increasing sputtering current. As the sputtering current was increased

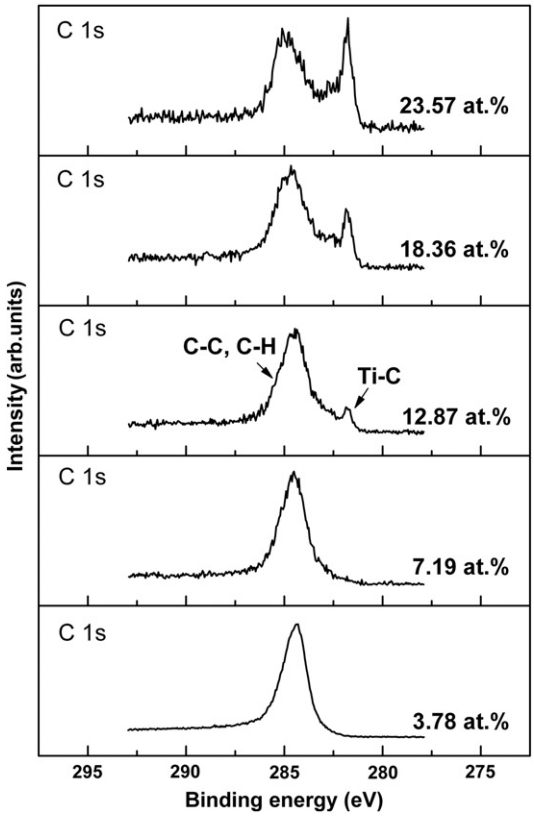

Fig. 2. Typical XPS C 1s peaks of the films with various Ti contents.

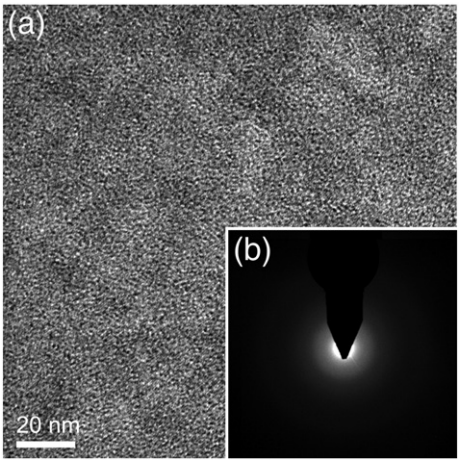

Fig. 3. (a) A TEM micrograph and (b) corresponding SAED pattern of the Ti-DLC films with 7.19 at.% Ti.

from 2 A to 3 A, the Ti content in the films varied from <4 to >23 at.%. This indicates that the Ti content in the films could be precisely controlled by adjusting the magnetron sputtering current in the hybrid ion beam deposition system. The growth rate of the films was also increasing monotonously from 13.5 to 19 nm/min by increasing the sputtering current from 2 A to 3 A, which was similar to the result obtained for Al-DLC films in our previous work, indicating that the metal incorporation improves the growth rate of the DLC films [20].

The chemical bonds of the deposited films were analyzed by the XPS spectra as shown in Fig. 2, where C 1s spectra of the deposited films were compared for various Ti contents. For the films with low Ti contents (<8 at.%), only a major peak at a binding energy of around 284.5 eV appeared, which represents the typical C–C or C–H binding energy of the DLC film [15]. As the Ti content increased to 12.87 at.%, a shoulder peak at a lower binding energy of 282 eV appeared, and the peak intensity increased with the increase of the Ti content. Taking into account that the binding energy of 282 eV is typical for Ti–C bonds, it can be deduced that titanium carbide was formed in the films and that the fraction of the carbide increased as the Ti content increased [21].

In order to obtain insight into the structure evolution of Ti-DLC films as a function of doped Ti content, a TEM measurement was made. Fig. 3 shows the TEM micrograph and corresponding selected area electron diffraction (SAED) pattern of the film with 7.19 at.% Ti. The TEM picture (Fig. 3(a)) presents dense and smooth granular contrasts, and the corresponding SAED (Fig. 3(b)) shows a broad and diffuse diffraction halo pointing out the typical amorphous feature as shown in the pure DLC [20]. This implies that the deposited film essentially formed a typical amorphous structure and the Ti atoms were uniformly distributed and dissolved in the DLC matrix. For the Ti-DLC film with Ti 18.36 at.%, it is characteristic to note that numerous nanoparticles are presented in the film as shown in Fig. 4 (a). A magnified image (Fig.4 (b)) reveals the clear lattice fringes of the nanoparticles (noted by the red circles) uniformly embedded in the DLC matrix, and the typical sizes of the crystal domains are about 5 nm in diameter. Furthermore, the sharp crystalline diffraction rings observed in Fig. 4(c) indicate the existence of polycrystalline phases, which are identified to be the (111), (200), and (220) reflections of the cubic (FCC) TiC structure. In this case, it could be concluded that the titanium carbide crystalline phase was formed in the DLC films at relatively high content Ti doping.

Compared with Ti-DLC films fabricated using different deposition techniques reported elsewhere, the formation of the carbide nanoparticles is significantly different if one notes the solubility of the doped Ti atoms in the DLC matrix. The dissolution threshold of Ti atoms in the DLC films deposited by the reactive magnetron sputtering technique was reported to 0.9 and 2.5 at.% [22]. Beyond this solubility range, nanocrystalline carbides could be observed in the films. However, Zhang et al. [15] synthesized Ti-DLC films via the co-sputtering of graphite and titanium targets, and found that nanocrystalline TiC started to emerge in the amorphous DLC matrix as the Ti content increased up to 16 at.%, which is relatively higher than the result found in the present work, where the Ti solubility in the films was suggested to lie between about 7 and 13 at.% according to the XPS and TEM results. The above difference in the obtained Ti solubility for Ti-DLC films was attributed to the process parameters, which should be discussed in later work.

Raman spectroscopy is a powerful tool for characterizing the detailed carbon bonding structure of the DLC films. Fig. 5(a) shows representative Raman spectra of the Ti-DLC films with various Ti contents. It is obvious that all the spectra display a broad asymmetric Raman scattering curve in the range of 1000–1700 cm^{-1}, which is the characteristic peak of the pure DLC films [1]. However, it should be noted that the intensity of the Raman spectra decreased as the doped Ti content in the films was increased, due to the decrease of the DLC fraction per unit area of the film. Normally, the Raman spectra of the DLC film can be fitted by the D peak around 1350 cm^{-1} and the G peak around 1550 cm^{-1} (as shown in an insert in Fig.5 (a)). The D peak is due to the breathing modes of only those sp^2 atoms that are in aromatic rings, and the G peak is derived from the bond stretching of all pairs of sp^2 atoms in both aromatic rings and chains [1]. Accordingly, the intensity ratio of the D peak to G peak (I_D/I_G) can be used to characterize the carbon atomic structure in DLC films. The intensity ratio, I_D/I_G, increases as the graphitic component (sp^2-C) increases in the films [1,23]. As shown in Fig. 5(b), the I_D/I_G of the films were reduced at

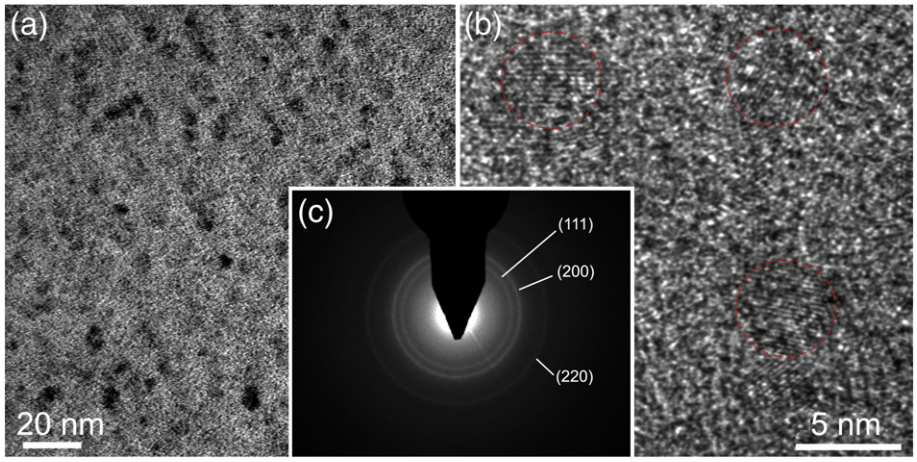

Fig. 4. TEM micrographs at (a) low and (b) high magnification and (c) corresponding SAED pattern of the Ti-DLC films with 18.36 at.% Ti.

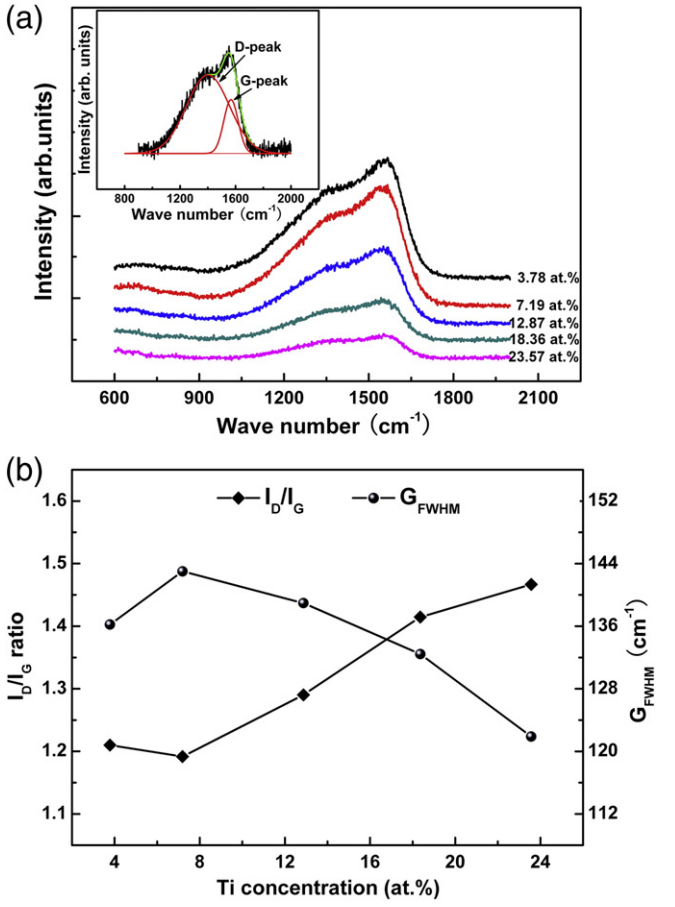

Fig. 5. (a) Representative Raman spectra, (b) corresponding I_D/I_G ratios and G_{FWHM} of the Ti-DLC films as a function of Ti content.

lower Ti contents, and increased monotonously with increasing Ti content. This result reveals that increasing the Ti content at first caused the fraction of sp^2-C bonds to decrease, but then it increased due to more graphitization. The full width at half maximum (FWHM) of the G peak (G_{FWHM}) can be also used to identify the degree of disorder of the carbon structure, since an decrease of G_{FWHM} accompanies the ordering and graphitizing of the DLC films [23]. As shown in Fig. 5(b), G_{FWHM} underwent an increase in response to the initial increase of Ti content, and then decreased monotonously when the Ti content exceeded 7.19 at.%. It could be therefore said that the fraction of sp^2-C decreased at first with the addition of Ti, but this was then followed by a monotonous

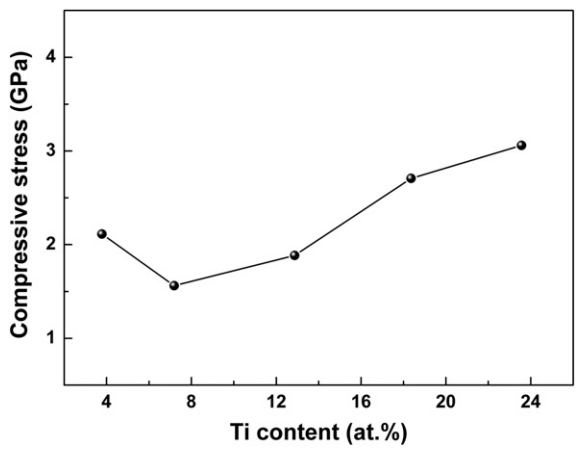

Fig. 6. Compressive stress of the Ti-DLC films as a function of Ti content.

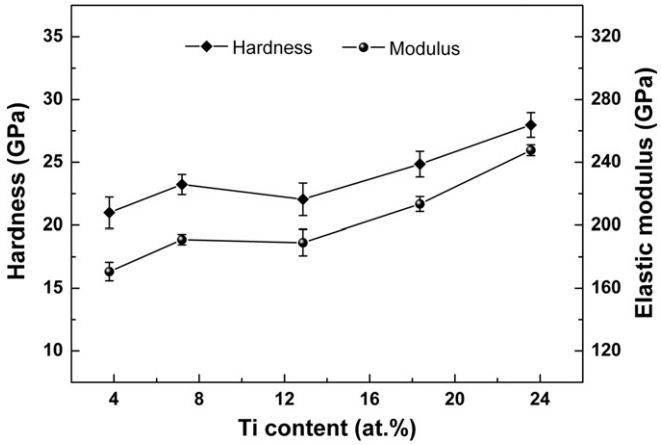

Fig. 7. Hardness and elastic modulus of the Ti-DLC films as a function of Ti content.

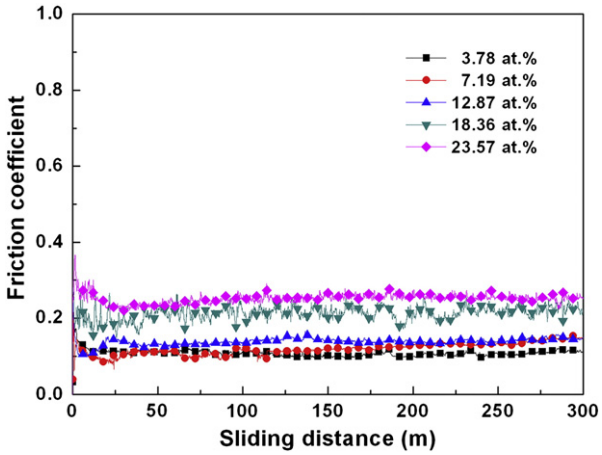

Fig. 8. Friction coefficient of the Ti-DLC films with various Ti contents as a function of sliding distance.

increase, displaying an increase of cluster ordering and graphitization, which agreed well with the results of I_D/I_G. The achieved evolution of carbon atomic bonds as a function of the doped Ti content can be understood in terms of two factors. Firstly, the sp^2-C bond has relatively lower bonding energy than that of the sp^3-C, which makes it favorable to bond with

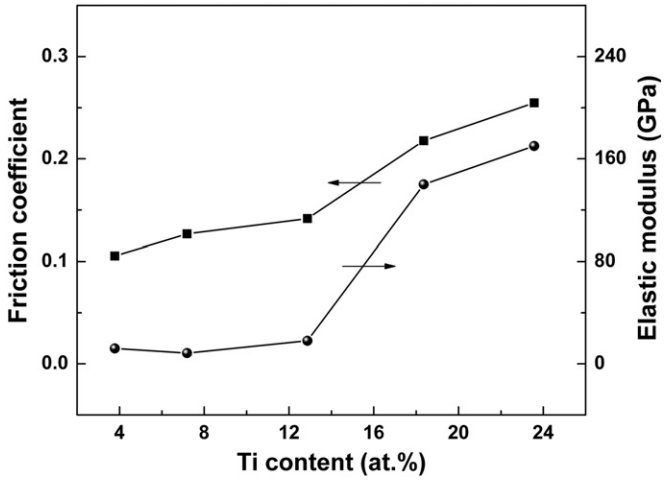

Fig. 9. Average friction coefficient and wear rate of the films as a function of Ti content.

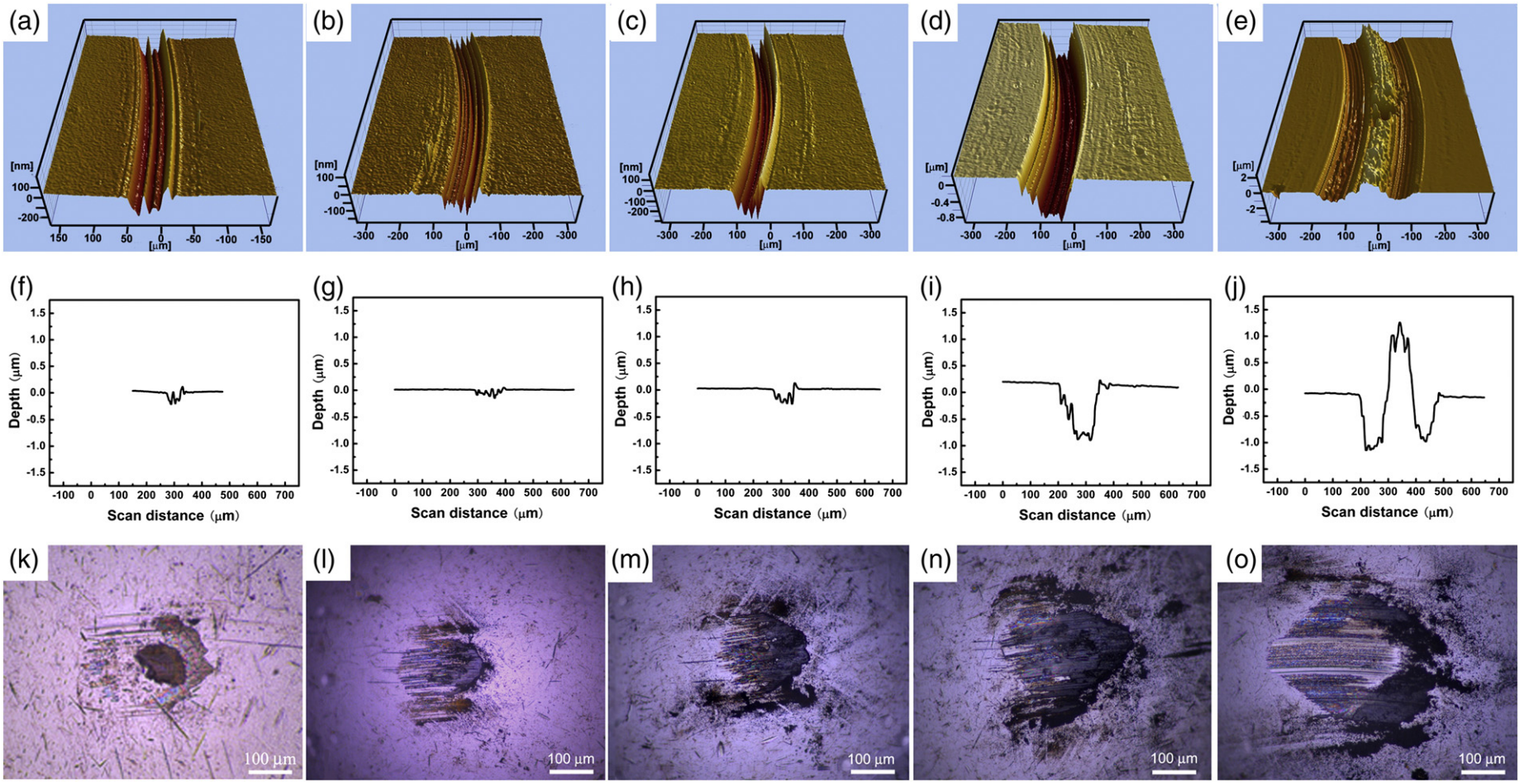

Fig. 10. 3D scanning morphologies (top row) and cross-section surface profiles (mid) of the wear tracks and optical micrographs (bottom) of the corresponding contact ball of the films: (a), (f) and (k) 3.78 at.%; (b), (g) and (l) 7.19 at.%; (c), (h) and (m) 12.87 at.%; (d), (i) and (n) 18.36 at.%; and (e), (j) and (o) 23.57 at.%.

the doped metal atoms and form the nano-crystalline carbide. As a consequence, the sp^2-C bond fraction in the film was decreased at lower doped Ti content. However, the doped Ti metal atoms forming the carbide acted as a catalyst to promote graphitization, where the formed metal carbide crystallites were surrounded by an increased number of sp^2-C bonds [24,25]. These films displayed a nanocomposite structure with nanoparticles embedded in the amorphous carbon matrix. As a result, the films tended to be graphitized for increased levels of Ti incorporation.

The in-plane compressive stress and mechanical properties of the films were measured as a function of the Ti content in Fig. 6 and 7. A lower compressive stress of about 2.2 GPa was measured for the Ti-DLC film with Ti 3.78 at.% compared with the pure DLC film, which had a stress of about 2.7 GPa [20]. As the Ti content increased up to ~7 at.%, the compressive stress of the film dramatically dropped down to 1.5 GPa, whereas it subsequently increased to 3 GPa as the Ti content reached to ~24 at.%. Wang et al. [26] proposed that the metal atoms dissolved in the amorphous carbon matrix play the role of pivotal sites, where distortion of the atomic bond angles could easily occur without inducing a significant increase in the elastic energy. The compressive stress could, therefore, be significantly relaxed through the convenience of atomic bond distortion. According to the structural and compositional analysis, when the doped Ti content was less than 8 at.%, it could be said that the doped Ti atoms were uniformly dissolved in the amorphous DLC matrix and not bonded with C to form nano-crystalline carbides. The consequence was similar to that seen in W-DLC films [26]: the film with the low doped Ti content presented a relatively low compressive stress. However, as the Ti content exceeded the solubility level, the carbide phase of Ti–C started to evolve in the amorphous carbon matrix. Because the Ti–C bond length was longer than the C–C bond, the presence of Ti–C caused an increase of the compressive stress in the film.

The mechanical properties of hardness and elastic modulus of the Ti-DLC films were estimated as a function of the Ti content. The hardness of the films increased monotonously with increasing Ti content, except for the case with a Ti content of 12.87 at.%. Generally, the mechanical properties of DLC films mainly depend on the sp^3 carbon interlink matrix. According to the Raman results, the films tended to graphitize as the Ti content increased from 7.19 to 12.87 at.%, resulting in a decrease of the film hardness. However, in the case of high Ti content, a mass of hard titanium carbide nano-particles were formed and embedded in the DLC matrix, which significantly contributed to the increase of the film hardness. Accordingly, the films displayed high hardness values of around 28 GPa and an elastic modulus of 247.7 GPa at the high doped Ti content of about 24 at.%. This result is different from the observation that the hardness decreases in response to increasing the content of a doped metal that cannot form the hard carbide phase embedded in the amorphous matrix, such as in the Al-DLC films that were also deposited by the hybrid ion beam system [20].

In order to investigate the friction and wear behavior of the deposited Ti-DLC films, tribological tests were performed. The friction coefficient of the films as a function of sliding distance was shown in Figs. 8, and Fig. 9 illustrates the average friction coefficients and wear rate with the Ti content. It can be seen that the films containing low Ti content (<8 at.%) presented a relatively steady and low friction coefficient lower than 0.13. And the wear rates of the films were also very low, not higher than 1.2×10^{-7} mm^3/N-m. However, further increasing the Ti content, the friction coefficient and wear rate of the films increased sharply, and they reached to the high values of about 0.25 and 1.7×10^{-6} mm^3/N-m respectively, when the Ti content increased up to ~24 at.%. Fig. 10 shows the micrographs and corresponding cross-section profiles of the film wear tracks and the wear scars on the counter ball after the friction test. The films with low Ti content (<8 at.%) revealed smooth wear tracks with low wear depths (<200 nm). The corresponding counter balls also presented small wear scars, the sizes of which were lower than 150 μm. As the Ti content increased, the wear track became wider and deeper, and the wear scar on the ball was also enlarged with the increased appearance of an adherent transfer layer. When the Ti content reached up to 18.36 at.%, the wear depth of the film and the size of the wear scar on the ball increased to about 0.9 μm and 300 μm, respectively.

The DLC film with high Ti content 23.57 at.% reveals a unique wear track with a "W" shape as shown in Fig. 10 (e). To clarify this strange phenomenon, SEM and EDS were used to analyze the wear track in the film carefully, as shown in Fig. 11. A mass of wear debris was found to accumulate in the prominent area (the B-area shown in Fig. 11 (c)), but the concave area was very clean without any wear debris (the A-area shown in Fig. 11 (a)). Compositional analysis of EDS on the A-area and the B-area (Fig. 11 (d)) showed that a large amount of Fe was observed on the B-area. It is obvious that the Fe element was dominantly transferred from the counter steel ball, causing a serious wear as shown in Fig. 10 (o).

The observed friction and wear behaviors of the Ti-DLC films can be understood in terms of the microstructure evolution as a function of the doped Ti content. For the films with low doped Ti content, the doped Ti atoms mainly dissolved in the amorphous DLC matrix, and the film exhibited the features of an amorphous carbon structure and thus displayed a low friction coefficient and wear rate. However, for the films with high doped Ti content, the hard titanium carbide nanoparticles started to emerge in the DLC matrix and both their fraction and size increased, so that the amorphous DLC film was gradually transformed into a carbide-rich film. This result would cause abrasive wear and thus deteriorate the wear performance, as verified by the obtained high friction coefficient and wear rate.

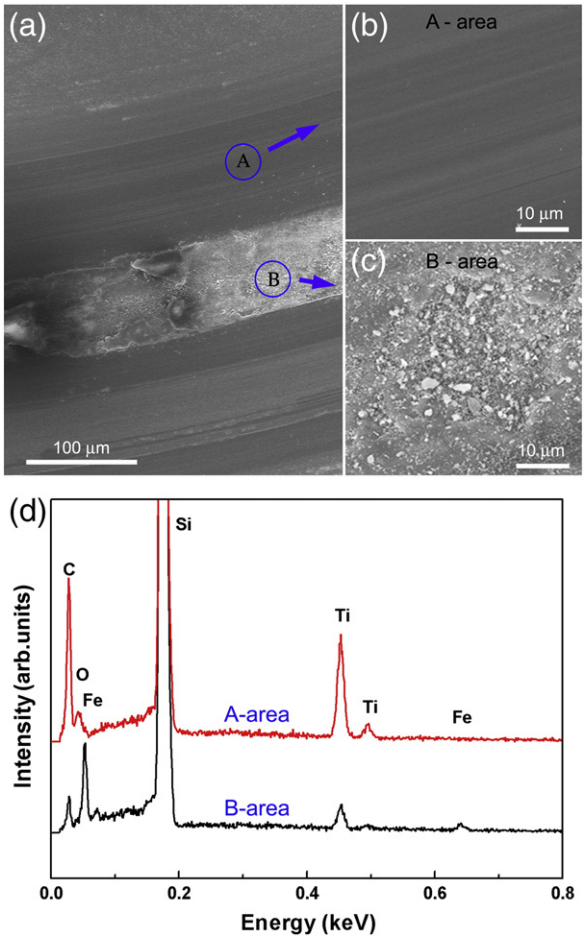

Fig. 11. (a) An SEM image of the wear trace on the Ti-DLC film with 23.57 at.% Ti. The magnified images of the (b) A-area and (c) B-area from (a), and (d) EDS profiles on the A-area and B-area.

4. Conclusions

Ti-DLC films with Ti contents varying up to 24 at.% were deposited by a hybrid ion beam system consisting of an anode-layer linear ion source and a DC magnetron sputtering source. Compositional and structural analysis showed that the maximum solubility of the doped Ti atoms in the films was proposed to lie between about 7 and 13 at.%. When the Ti content was less than this solubility, the doped Ti atoms were uniformly dissolved in the amorphous hydrogenated carbon matrix, so that the films exhibited the dominant features of the pure DLC structure and experienced a significant reduction in the compressive stress, as well as a lower friction coefficient and wear rate. As the Ti content exceeded the solubility, the doped Ti atoms bonded with the surrounding C atoms, and subsequently formed carbide nano-particles that were embedded in the DLC matrix. The bonding of Ti and C would increase the film compressive stress owing to the bond length difference between Ti–C and C–C. Whereas the hard carbide nano-particles could significantly enhance the hardness of the films, they also promoted the graphitization of films due to the catalysis effect. On the other hand, it was observed that the formed hard carbide nano-particles caused abrasive wear and resulted in a high friction coefficient and wear rate of the films.

Acknowledgements

This work was financially supported by the State Key Project of Fundamental Research of China (Grant No: 2012CB933003) , the project of the Natural Science Foundation of China (Grant No: 51072205) and State Key Lab of Solid Lubrication from Lanzhou Institute of Chemistry and Physics, in part by the internal project of KIST and TES Co. Ltd. under the 'Advanced Manufacturing Technology Research Center' Program of the MKE of Korea.

References

[1] J. Robertson, Mater. Sci. Eng., R 37 (2002) 129.
[2] R. Hauert, Tribol. Int. 37 (2004) 991.
[3] J. Robertson, Jpn. J. Appl. Phys. 50 (2011) 01AF01.
[4] M. Lejeune, M. Benlahsen, R. Bouzerar, Appl. Phys. Lett. 84 (2004) 344.
[5] G. Gassner, P.H. Mayrhofer, C. Mitterer, J. Kiefer, Surf. Coat. Technol. 200 (2005) 1147.
[6] G. Gassner, P.H. Mayrhofer, J. Patscheider, C. Mitterer, Thin Solid Films 515 (2007) 5411.
[7] Y. Pauleau, E. Thiery, Surf. Coat. Technol. 180 (2004) 313.
[8] K.I. Schiffmann, Surf. Coat. Technol. 177 (2004) 453.
[9] V. Singh, J.C. Jiang, E.I. Meletis, Thin Solid Films 189 (2005) 150.
[10] P. VijaiBharathy, D. Nataraj, Paul K. Chu, Huaiyu Wang, Q. Yang, M.S.R.N. Kiran, J. Silvestre-Albero, D. Mangalaraj, Appl. Surf. Sci. 257 (2010) 143.
[11] W. Gulbinski, S. Mathur, H. Shen, T. Suszo, A. Giewicz, B. Warcholinski, Appl. Surf. Sci. 239 (2005) 302.
[12] R. Hauert, Diamond Relat. Mater. 12 (2003) 583.
[13] X.L. Bui, Y.T. Pei, J.Th.M. De Hosson, Surf. Coat. Technol. 202 (2008) 4939.
[14] W.J. Meng, E.I. Meletis, L.E. Rehn, P.M. Baldo, J. Appl. Phys. 87 (2000) 2840.
[15] S. Zhang, X.L. Bui, J. Jiang, X. Li, Surf. Coat. Technol. 198 (2005) 206.
[16] D. Caschera, F. Federici, S. Kaciulis, L. Pandolfi, A. Cusma, G. Padeletti, Mater. Sci. Eng., C 27 (2007) 1328.
[17] A. Anders, Surf. Coat. Technol. 200 (2005) 1893.
[18] W. Dai, A. Wang, Surf. Coat. Technol. 205 (2011) 2882.
[19] W. Dai, H. Zheng, G. Wu, A. Wang, Vacuum 85 (2010) 231.
[20] W. Dai, A. Wang, J. Alloys Compd. 509 (2011) 4626.
[21] K. Baba, R. Hatada, Surf. Coat. Technol. 169–170 (2003) 287.
[22] W.J. Meng, R.C. Tittsworth, L.E. Rehn, Thin Solid Films 377–378 (2000) 222.
[23] C. Casiraghi, A.C. Ferrari, J. Robertson, Phys. Rev. B 72 (2005) 085401.
[24] K. Bewilogua, R. Wittorf, H. Thomsen, M. Weber, Thin Solid Films 447–448 (2004) 142.
[25] A.A. Voevodin, M.A. Capano, S.J.P. Laube, M.S. Donley, J.S. Zabinski, Thin Solid Films 298 (1–2) (1997) 107.
[26] A.Y. Wang, K.R. Lee, J.P. Ahn, J.H. Han, Carbon 44 (2006) 1826.